Application of a unified theory of rearrangement scattering to (p,d) reactions

J. M. Greben
Department of Physics, University of Alberta, Edmonton, Alberta, Canada T6G 2J1
(Received 11 October 1983)

In a recently developed many-body Faddeev theory of rearrangement scattering the transition matrix elements are given in terms of a distorted wave series. We discuss the construction of the distorted waves and evaluate the lowest order contribution to $^{24}Mg(\vec{p},d)^{23}Mg$ at 96 MeV in zero range. Various approximations are examined and possible extensions of the present calculations are discussed.

[NUCLEAR REACTIONS Intermediate energy (p-d) reactions. Application of microscopic theory of rearrangement scattering. Calculation of distorted waves.]

I. INTRODUCTION

Since the first (p,d) experiments at intermediate energy were performed at Saclay[1] in 1974, there has been a growing interest in this reaction at medium energies, both from the experimental[2–10] and the theoretical side.[11–18] Although one can use this reaction at intermediate energies as a conventional nuclear structure tool, e.g., by exploring deeply bound hole states in the nucleus, the main motivation for this renewed interest lies in the hope of obtaining new types of information with this reaction at higher energies. In particular, one hopes[1,2,6,8,9,11] that this reaction will provide information on the high momentum components of the transferred nucleon wave function, which to some extent will reflect the high momentum distribution of the nuclear wave function. Unfortunately, very little information has been obtained so far about high momentum components, although there are encouraging signs that the process is sensitive to such components.[13] The problem is that at these high momentum transfers rescattering terms—which serve to distribute the momentum transfer over various steps and therefore do not excite high momentum components—become important. These rescattering terms can show up in various ways, e.g., as continuum effects which increase in importance with increasing energy,[19,20] or as explicit rescattering diagrams involving two[6,9] or more target nucleons or even pion and isobar degrees of freedom.[11,17] It should be obvious that problems of overcounting arise if several mechanisms are included simultaneously. Hence, in order to obtain quantitative information from these transfer experiments one has to treat the direct and rescattering terms in a unified way.

In a previous paper[21] we developed such a unified theory which incorporates all conventional nucleonic diagrams in a distorted wave series. The theory has a Faddeev-type structure and exploits standard projection techniques to eliminate explicit reference to all but the two asymptotic channels. Two expansions characterize the distorted wave series: first, a coupled channel expansion of the full amplitude in terms of the coupling potentials, and second, an expansion of the coupling potentials themselves. Based on previous experience with three-body model studies, we expect that the first expansion converges rapidly so that the higher-order recoupling terms can be neglected. The convergence of the expansion of the coupling potential, which includes rescattering terms and contributions of various inelastic excitations, is less obvious. The idea behind a distorted wave series is that the major contributions from rescattering and inelastic channels are absorbed into the distorted waves, so that the remaining transition operator can be approximated by a few low-order terms. Since the present theory gives a natural and rigorous definition of the distorted waves, based on the exact three-cluster equations, we expect that it gives an optimal realization of this intuitive idea so that the convergence properties are optimized. More specifically, the higher-order terms in the coupling potentials have two desirable features: first, they are expressed in terms of intercluster t matrices which are better behaved than potentials, and second, they are suppressed by the restriction to intermediate Q states (except for one special rescattering term). Naturally, the ultimate test of the convergence properties should come from explicit calculations.

The purpose of this paper is to demonstrate the practicality of the present microscopic approach and to assess the value of the lowest-order approximation. We found in earlier three-body model studies that the distorted waves play a very important role in the prediction of the observables, so that it is natural to first study the effects of the modifications of the distorted waves as required by the present theory. In subsequent work we could then examine the role of the special rescattering term, and draw conclusions about the convergence of the series.

The outline of the paper is as follows. In Sec. II we briefly summarize the unified theory of rearrangement scattering. In Sec. III we develop approximations for the distorted waves and in Sec. IV we present our results and comparison with the standard DWBA. Finally, in Sec. V we discuss our results and present our major conclusions.

II. DESCRIPTION OF (p,d) REACTIONS IN THE UNIFIED MICROSCOPIC THEORY

In this section we summarize the equations of the unified theory of rearrangement scattering of Ref. 21 relevant for the *direct* (p,d) amplitude (see Fig. 1). The exchange amplitude can be dealt with in a similar manner; however, the physical approximations and the required nuclear structure information are slightly different, as we deal with different dynamics. For forward (p,d) scattering the direct amplitude is expected to dominate and we expect to be able to describe the experimental data reasonably well with this amplitude alone. We assume that the dynamics of the system is governed by the nonrelativistic $(A+1)$-body Hamiltonian:

$$H=\sum_{i=0}^{A} T_i+\sum_{i<j}^{A} V_{ij} \ . \tag{2.1}$$

Using a Faddeev decomposition of the wave function corresponding to the three-body dynamics of the direct process, and by projecting out the relevant asymptotic channels using standard Feshbach projectors,[22] we arrive at the following expression for the direct scattering amplitude:[21]

$$\langle \Psi_B \Psi_d \vec{k}' \mid T^{\rm dir} \mid \Psi_A \vec{k} \rangle = \langle \Psi_B \Psi_d \hat{\chi}^{(-)}_{3,\vec{k}'} \mid T_{31} \mid \Psi_A \hat{\chi}^{(+)}_{1,\vec{k}} \rangle \ . \tag{2.2}$$

Channels are labeled by indices $i=1,2,3$, where 1 stands for the proton channel, 3 for the deuteron channel, and 2 for the suppressed neutron channel. The distorted waves are characterized by a channel index and a wave vector $\vec{k}$. They can be expressed in terms of the elastic wave functions by

$$\hat{\chi}^{(+)}_{i,\vec{k}}(\vec{r})=\chi^{F(+)}_{i,\vec{k}}(\vec{r})-\int d\vec{r}\,' \langle \vec{r} \mid \langle G_0 U_i^F \rangle \mid \vec{r}\,' \rangle \chi^{F(+)}_{i,\vec{k}}(\vec{r}\,') \ , \tag{2.3}$$

where G_0 will be defined later. The elastic wave function is defined by the Schrödinger equation

$$(E+E_i-K_i-\langle U_i^F \rangle)\chi^{F(+)}_{i,\vec{k}}=0 \ , \tag{2.4}$$

with the usual boundary condition for incoming waves. We denote the threshold energy by E_i and the kinetic energy operator for the relative motion by K_i. The optical potential $\langle U_i^F \rangle$ is the ground-state matrix element of the Feshbach optical potential operator. For the proton channel this optical potential operator is given by

$$U_1^F=\sum_{i=1}^{A} V_{0i}+U_1^F Q_1 (E-H_1+i\epsilon)^{-1} \sum_{i=1}^{A} V_{0i} \ , \tag{2.5}$$

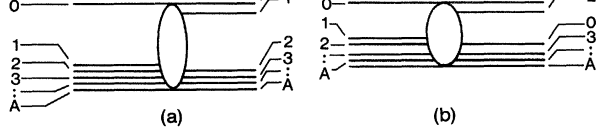

FIG. 1. Direct and exchange amplitudes for the (p,d) reaction.

where Q_1 is the projection operator which excludes the target state of nucleus A. The channel Hamiltonian H_1 is defined by

$$H_1=\sum_{i=0}^{A} T_i+\sum_{\substack{i<j \\ i\neq 0}}^{A} V_{ij} \ . \tag{2.6}$$

The microscopic deuteron optical potential operator is given by

$$U_3^F=\sum_{i\geq 2}^{A} (V_{0i}+V_{1i}) + U_3^F Q_3 (E-H_3+i\epsilon)^{-1} \sum_{i\geq 2}^{A} (V_{0i}+V_{1i}) \ , \tag{2.7}$$

where

$$H_3=\sum_{i=1}^{A} T_i+V_{01}+\sum_{1<i<j}^{A} V_{ij} \ . \tag{2.8}$$

The projection operator Q_3 excludes states which can be written as a product of the deuteron and residual nucleus ground state.

In Eq. (2.3) we also introduce the three-body Green's function G_0:

$$G_0(E)=(E-H_0+i\epsilon)^{-1} \ , \tag{2.9}$$

where

$$H_0=\sum_{i=1}^{A} T_i+\sum_{1<i<j} V_{ij} \tag{2.10}$$

is the channel Hamiltonian for the three-body breakup channel with clusters p, n, and B. Since G_0 can connect two-body cluster wave functions with three-body cluster wave functions, $2\rightarrow 3$ matrix elements of U_i^F are required in Eq. (2.3). However, we will see in the next section that we can develop reasonable approximations which only require the knowledge of the optical potential $\langle U_i^F \rangle$, despite the presence of G_0.

We now briefly review the expansion of the transition operators. As shown in Ref. 21, we can expand these operators in a coupled channel series

$$\hat{T}_{ji}=P_j(V_j+U_{ji})P_i-\hat{T}_{ji}P_i\hat{G}_i(V_i+U_{ij})P_j\hat{G}_j\hat{T}_{ji} \ , \tag{2.11}$$

where $P_j(V_j+U_{ji})P_i$ is the *transition potential.* The Green's function $\hat{G}_i$ is defined in terms of the distorting potential $\hat{U}_{ii}$ (the potential which generates the distorted waves $\hat{\chi}^{(\pm)}_{i,\vec{k}}$):

$$\hat{G}_i(E+i0)=(E-H_i-\langle \hat{U}_{ii} \rangle+i0)^{-1} \ , \tag{2.12}$$

so that $\hat{G}_i$ has the form of a free propagator in the distorted wave basis $\hat{\chi}_{i,\vec{k}_i}$. Therefore, it is possible to solve for the subsequent terms in Eq. (2.11) by an iterative set of coupled channel equations. One can show that $\langle \hat{T}_{ji} \rangle$ can be written in closed form as

$$\langle \hat{T}_{ji} \rangle = \langle V_j+U_{ji} \rangle [-\tfrac{1}{2}\hat{Z}_i^{-1}+\tfrac{1}{2}\hat{Z}_i^{-1}(1+4\hat{Z}_i)^{1/2}] \ , \tag{2.13}$$

where

$$\hat{Z}_i = P_i \hat{G}_i \langle V_i + U_{ij} \rangle P_j \hat{G}_j \langle V_j + U_{ji} \rangle \ , \quad i \neq j \ (1 \text{ or } 3) \ . \tag{2.14}$$

In Ref. 21 we argued that we expect the series (2.11) to converge rapidly. We will therefore concentrate on the expansion of the first term: the transition potential.

The transition potential can also be expanded, although no simple coupled channel series like (2.11) exists. The first term in the coupling potential $\langle V_j + U_{ji} \rangle$ is obviously $\langle V_j \rangle$, whose matrix element is the microscopic DWBA amplitude:

$$\langle \psi_B \psi_d \hat{\chi}^{(-)}_{3,\vec{k}'} | \, T_{31}^{(\mathrm{DWBA})} \, | \psi_A \hat{\chi}^{(+)}_{1,\vec{k}} \rangle = \langle \psi_B \psi_d \hat{\chi}^{(-)}_{3,\vec{k}'} | \, V_3 \, | \psi_A \hat{\chi}^{(+)}_{1,\vec{k}} \rangle \ . \tag{2.15}$$

The expansion of U_{31} is discussed in Ref. 21. The main rescattering term has the form

$$\langle \psi_B \psi_d \hat{\chi}^{(-)}_{3,\vec{k}'} | \, T_{31}^{\mathrm{resc}} \, | \psi_A \hat{\chi}^{(+)}_{1,\vec{k}} \rangle = \langle \psi_B \psi_d \hat{\chi}^{(-)}_{3,\vec{k}'} | \, V_3 G_0 T_2 \, | \psi_A \hat{\chi}^{(+)}_{1,\vec{k}} \rangle \ . \tag{2.16}$$

This mechanism is portrayed in Fig. 2. In Eq. (2.16) we introduced the T matrix T_2:

$$T_2 = V_2 + V_2 G_0 T_2 \ , \tag{2.17}$$

with

$$V_2 = \sum_{i \geq 2}^{A} V_{0i} \ . \tag{2.18}$$

Both the DWBA diagram and the rescattering graph will peak for small angles; however, their minima will not be at the same place, so that this rescattering term will wash out some of the structure inherent to the single pickup amplitude. Other terms in the driving term for U_{31} involve the excitation of the initial target, the excitation of two nucleons via the rescattering of the projectile proton, and target excitation combined with the rescattering process in Fig. 2. In the next section we will start the analysis of the distorted waves and their application to the first order diagram.

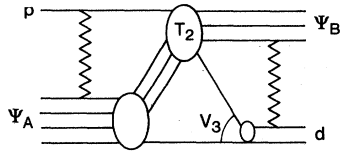

FIG. 2. Rescattering mechanism in the (p,d) reaction. Wiggly lines indicate the distortion of the relative wave functions.

III. EVALUATION OF THE DISTORTED WAVES

The distorted waves $\hat{X}_{i,\vec{k}_i}$ are defined in terms of the elastic wave functions $\hat{X}^F_{i,\vec{k}_i}$ through Eqs. (2.3). In order to determine the required matrix elements $\langle G_0 U_i^F \rangle$, it is convenient to expand the cluster states Ψ_d or Ψ_A in terms of eigenstates of the Hamiltonian H_0. In the proton case we have

$$| \Psi_A \rangle = \sum_{\mu} \int d\vec{p} \, f^1_\mu(\vec{p}) \, | \eta^\mu_B \vec{p} \rangle \ , \tag{3.1}$$

where η^μ_B is a complete set of eigenstates of the core. For the deuteron channel $| \Psi_B \rangle = | \eta^0_B \rangle$, and Ψ_d is the internal deuteron wave function. Consider the result for the proton case:

$$\langle \Psi_A \vec{r} \, | \, G_0 U_1^F \, | \, \Psi_A \vec{r}' \rangle = -\frac{M_1}{2\pi} \sum_{\mu} \int d\vec{p} \int \vec{dr}'' f^1_\mu(\vec{p})^* \frac{\exp\{i[2M_1(E + \epsilon^\mu_B - p^2/2\mu_1)]^{1/2} \, | \vec{r} - \vec{r}'' | \}}{| \vec{r} - \vec{r}'' |} \langle \eta^\mu_B \vec{p} \vec{r}'' \, | \, U_1^F \, | \, \Psi_A \vec{r}' \rangle \ . \tag{3.2}$$

Here M_1 is the relative mass in the proton channel ($M_1^{-1} = M_p^{-1} + M_A^{-1}$), μ_1 is the relative mass of the neutron-core system ($\mu_1^{-1} = M_n^{-1} + M_B^{-1}$), and ϵ^μ_B is the binding energy of the core state μ, so that the neutron separation energy is $\epsilon^\mu_{\mathrm{sep}} = \epsilon_A - \epsilon^\mu_B$. If $\epsilon^\mu_B - p^2/2\mu_1$ is replaced by a constant, then we can use (3.1) and recover the ordinary optical potential matrix element of U^F. A natural choice for

$$\epsilon^\mu_B - p^2/2\mu_1 = \epsilon_A - \epsilon^\mu_{\mathrm{sep}} - p^2/2\mu_1$$

is $\epsilon_A + \langle V_1 \rangle$, where $\langle V_1 \rangle$ is the average potential energy of the neutron in the nucleus [notice that the momentum space representation of $V_1 = H_1 - H_0$ is $-\epsilon^\mu_{\mathrm{sep}} - p^2/2\mu_1$, according to Eq. (3.1)]. With this closure approximation we can write

$$\langle \Psi_A \vec{r} \, | \, G_0 U_1^F \, | \, \Psi_A \vec{r}' \rangle \simeq -\frac{M_1}{2\pi} \int dr'' \frac{\exp ik_0 \, | \vec{r} - \vec{r}'' |}{| \vec{r} - \vec{r}'' |} \langle \Psi_A \vec{r}'' \, | \, U_1^F \, | \, \Psi_A \vec{r}' \rangle \ , \tag{3.3}$$

where

$$k_0^2=2M_1(E+\epsilon_A+\langle V_1\rangle)=k^2+2M_1\langle V_1\rangle\ . \tag{3.4}$$

Although the microscopic optical potential $\langle U_1^F\rangle$ is nonlocal, in most applications of multiple scattering theory a local approximation is made. A local form should be even more justified in the present case, since U_1^F represents only the direct part of the potential and does not include the knockon term. For a local potential Eq. (3.3) reduces further, and using (2.3) we write the wave function as follows:

$$\hat{\chi}_{1,\vec{k}}(\vec{r})=\chi^F_{1,\vec{k}}(\vec{r})+\frac{M_1}{2\pi}\int d\vec{r}\,'\frac{e^{ik_0|\vec{r}-\vec{r}\,'|}}{|\vec{r}-\vec{r}\,'|}\times U_1^F(\vec{r}\,')\chi^F_{1,\vec{k}}(\vec{r}\,')\ . \tag{3.5}$$

The nature of the correction to $\chi^F_{1,\vec{k}}(\vec{r})$ can be illuminated by considering the special case $k_0=k$ (i.e., $\langle V_1\rangle=0$), which can also be considered as the extreme high-energy limit. In this case the correction cancels the scattering wave portion of $\chi^F_{1,\vec{k}}(\vec{r})$, and $\hat{\chi}_{1,\vec{k}}(\vec{r})$ becomes an ordinary plane wave. Intuitively, it is not unreasonable that at very high energies distortion effects become less important, and that the emphasis shifts away from distortion effects to individual direct processes represented in $\hat{T}_{ij}$.

The other extreme is that of strong binding and low energy. If we consider the momentum space verison of Eq. (3.2), then the relevant quantity to consider is the Green's function denominator $E+\epsilon_A-k^2/2M_1+V_1$, where we have substituted V_1 for $-\epsilon^{\mu}_{\rm sep}-p^2/2\mu_1$. For on-shell momenta [i.e., $k^2=2M_1(E+\epsilon_A)$] only V_1 survives, and if we replace this again by a constant $\langle V_1\rangle$ we obtain

$$\hat{\chi}_{1,k}(\vec{r})=[1-U_1^F(\vec{r})/\langle V_1\rangle]\chi^F_{1,\vec{k}}(\vec{r})\ . \tag{3.6}$$

The range of k being off shell is basically determined by the falloff of $U_F(|\vec{k}-\vec{k}\,'|)$. Consequently, Eq. (3.6) can only be valid if $|\langle V_1\rangle|$ is much larger than this spread in the momenta, i.e., we must satisfy the conditions

$$-\langle V_1\rangle\gg E+\epsilon_A \text{ and } -\langle V_1\rangle\gg\frac{1}{2M_1}\left[\frac{2\pi}{R_{\rm rms}}\right]^2, \tag{3.7}$$

where $2\pi/R_{\rm rms}$ characterizes the range of $U_1^F(q)$ in the momentum transfer q (for a Woods-Saxon potential it may be better to characterize this range by $1/a$). Since $\langle V_1\rangle$ and $U_1^F(\vec{r})$ are both negative at small energies, Eq. (3.6) entails a certain damping of the distorted waves in the nuclear interior. This could possibly explain the success[23] of cutoffs in DWBA calculations at low energies. Under the conditions of (3.7) one could also expand $\hat{\chi}_{1,k}(\vec{r})$ to higher order in $U_1^F(\vec{r})/\langle V_1\rangle$. The result then suggests the following Padé approximant:

$$\hat{\chi}_{1,\vec{k}}(\vec{r})=[1+U_1^F(\vec{r})/\langle V_1\rangle]^{-1}\chi^F_{1,\vec{k}}(\vec{r})\ . \tag{3.8}$$

In practice, we find that the approximations leading to (3.8) are unjustified, although expression (3.8) still has some value for illustrating the effect of smooth radial cutoffs in the DWBA integrals.

Although (3.6) and (3.8) are both approximations to (3.5), they share a property[21] with the exact wave function $\hat{\chi}_{1,\vec{k}}(\vec{r})$ which is absent in (3.5), namely, they are phase equivalent with $\chi^F_{1,\vec{k}}(\vec{r})$. The correction term in Eq. (3.5) contains outgoing waves of the form e^{ik_0r}/r which are suppressed in approximations (3.6) and (3.8). This shortcoming of Eq. (3.5) should not concern us too much, as the (p,d) amplitude is mainly sensitive to the distorted waves in the nuclear interior and the nuclear surface.

We now discuss the deuteron distorted wave. Instead of Eq. (3.2), we have

$$\langle\Psi_d\eta_B^0\vec{r}\,|\,G_0U_3^F\,|\,\Psi_d\eta_B^0\vec{r}\,'\rangle=-\frac{M_3}{2\pi}\int d\vec{p}\,\Psi_d(\vec{p})^*\int d\vec{r}\,''\frac{\exp\{i[2M_3(E+\epsilon_B^0-p^2/2\mu_3)]^{1/2}|\vec{r}-\vec{r}\,''|\}}{|\vec{r}-\vec{r}\,''|}\times\langle\eta_B^0\vec{p}\,\vec{r}\,''\,|\,U_3^F\,|\,\eta_B^0\Psi_d\vec{r}\,'\rangle\ . \tag{3.9}$$

The average potential energy of the nucleons in the deuteron is rather small ($\simeq$15 MeV), so that our analysis based on Eq. (3.5) suggests that $\hat{\chi}_{3,\vec{k}}(\vec{r})$ is intermediate between a plane wave and the normal elastic wave function. We would like to exploit our knowledge of the deuteron wave function so as to avoid closure approximation (3.3). Unfortunately, the deuteron optical potential complicates the analysis, as U_3^F is not known very well. In first approximation U_3^F is simply the sum of the proton and neutron optical potentials, and $\langle U_3^F\rangle$ is the folding potential. This approximation to U_3^F enables us to calculate the right-hand side of (3.9) exactly. We will use this approximation in the present study, although we should bear in mind that it has often been argued that breakup effects—which are neglected in the folding approximation—are important in deuteron elastic scattering. We obtain

$$\langle\Psi_d\eta_B^0\vec{r}\,|\,G_0U_3^F\,|\,\Psi_d\eta_B^0\vec{r}\,'\rangle=\frac{M_3}{2\pi\rho}\int d\vec{p}\int d\vec{q}\,\Psi_d(\vec{p})^*\exp\{i[2M_3(E+\epsilon_B^0-p^2/2\mu_3)]^{1/2}\}\times\Psi_d(\vec{p}+\vec{q}/2)[e^{-i\vec{r}\,''\cdot\vec{q}}U_p(\vec{q})+e^{-i\vec{r}\,''\cdot\vec{q}}U_n(-\vec{q})]\ , \tag{3.10}$$

where $\rho=|\vec{r}-\vec{r}'|$. In deriving (3.10) we assumed that the proton and neutron optical potentials are local. In practice one takes the nucleon optical potentials at half the deuteron energy. We have not dealt explicitly with the spin dependence of the nucleon and deuteron potentials. Such spin dependence complicates the analysis considerably without providing much new insight. In the same notation the folded deuteron potential reads

$$U_3^F(\vec{r})=\int d\vec{q}\int d\vec{p}\,\Psi_d(\vec{p})^*\Psi_d(\vec{p}+\vec{q}/2)[U_p(\vec{q})e^{-i\vec{r}\cdot\vec{q}}+U_n(-\vec{q})e^{i\vec{r}\cdot\vec{q}}]$$
$$=2\int d\vec{q}\,\rho_d(q/2)U_p(\vec{q})e^{-i\vec{r}\cdot\vec{q}}\ , \tag{3.11}$$

where

$$\rho_d(q)=\int d\vec{r}\,e^{i\vec{r}\cdot\vec{q}}\,|\Psi_d(\vec{r})|^2 \tag{3.12}$$

is the Fourier transform of the deuteron density. In (3.11) we assumed that $U_n(\vec{q})=U_p(\vec{q})=U_p(q)$. To facilitate the analysis of (3.10) we introduce the quantity $p^2(\rho,r')$, defined by

$$\langle\Psi_d\eta_B^0\vec{r}\,|\,G_0U_3^F\,|\,\Psi_d\eta_B^0\vec{r}'\rangle=-\frac{M_3}{2\pi\rho}\exp(i\{2M_3[E+\epsilon_B^0-p^2(\rho,r')]/(2\mu_3)\}^{1/2})U_3^F(\vec{r}')\ . \tag{3.13}$$

A near constant value of $p^2(\rho,r')$ would justify closure approximation (3.3), with

$$\langle V_3\rangle=-\epsilon_d-\langle p^2(\rho,r')\rangle/2\mu_3\ ,$$

where ϵ_d is the deuteron binding energy.

We have applied the theory to the reaction ^{24}Mg$(\vec{p},d)^{23}$Mg$(\frac{1}{2}^+)$ at 96 MeV. This process has recently been measured[10] and has attracted a lot of theoretical interest.[24,25] A large discrepancy between standard DWBA calculations and experiment was observed which could not be explained by the coupling to the 2^+ states in ^{24}Mg,[24] or by the effects of break up.[25] Since a cutoff of the radial integrals leads to an improved description, it would seem that our theory, which under approximation (3.6) suggests a suppression of the nuclear interior, might provide a better description of the process and give a justification for the cutoff. In order to obtain the folded deuteron optical potential we need proton optical potentials off ^{23}Mg$(\frac{1}{2}^+)$. Lacking such potentials we have used proton optical potentials off ^{24}Mg at 50 MeV from the compilation of Perey and Perey,[26] with the following parameters: $V=43.6$, $r=1.09$, and $a_R=0.74$; $W=7.39$, $r_I=1.53$, and $a_I=0.533$. The real and imaginary potentials have rms radii of 3.67 and 3.95 fm, respectively. For the deuteron we use the S state Reid soft core wave function. In Table I we list $p^2(\rho,r')$ for a set of ρ and r' values. We see that Re$[p^2(\rho,r')]$ is always smaller than the expectation value of p^2 in the S state. Also, $p^2(\rho,r')$ has a negative imaginary part, which translates into a (slow) exponential decay of the effective Green's function.

If one wants to use an average value of $p^2(\rho,r')$ in $\langle V_3\rangle$ then one probably should use a value near the nuclear surface, since this is the region which is most important for the (p,d) reaction. An appropriate value is $p^2(\rho,r')=(0.230,-0.047)$ corresponding to $r'=4$ fm and $\rho=1.4$ fm. If one wants to improve beyond this approximation one should incorporate the p and/or r' behavior in integral (2.3). In order to do this we consider the large energy expansion of the modified Green's function in (3.13), which symbolically can be written as the two-body propagator

TABLE I. Listing of real and imaginary parts of $p^2(\rho,r')$ in fm^{-2}. The expectation value of the kinetic energy in the relative S state is 0.324 fm^{-2}. The first row contains the values $p^2(\rho)$ obtained by defining the effective Green's function [Eq. (3.13)] in terms of $\langle\Psi_d\eta_B^0\vec{r}\,|\,G_0\,|\,\Psi_d\eta_B^0\vec{r}'\rangle$.

r' \ ρ	0.2		0.6		1.4		3		6.2	
	0.246	−0.057	0.226	−0.048	0.211	−0.057	0.179	−0.071	0.138	−0.076
0.4	0.292	−0.073	0.274	−0.061	0.253	−0.071	0.217	−0.087	0.171	−0.094
2.0	0.304	−0.077	0.284	−0.066	0.261	−0.076	0.221	−0.093	0.171	−0.098
3.0	0.297	−0.070	0.277	−0.059	0.255	−0.070	0.216	−0.087	0.167	−0.093
4.0	0.265	−0.045	0.248	−0.036	0.230	−0.047	0.198	−0.065	0.156	−0.074
5.0	0.204	−0.028	0.191	−0.020	0.179	−0.027	0.158	−0.040	0.130	−0.048
7.0	0.089	−0.040	0.082	−0.034	0.073	−0.036	0.055	−0.036	0.038	−0.024

$$\langle \vec{r}' \mid G_3[E-\epsilon_d-p^2(\rho,r')/2\mu_3] \mid \vec{r}' \rangle = \langle \vec{r} \mid G_3[E-\epsilon_d-\langle p^2(\rho,r')\rangle/2\mu_3] \mid \vec{r}' \rangle \times \left\{ 1+\frac{i\rho\sqrt{2M_3}}{2} \frac{-p^2(\rho,r')+\langle p^2(\rho,r')\rangle}{[E-\langle p^2(\rho,r')\rangle]^{1/2}}+\cdots \right\} . \tag{3.14}$$

For large ρ ($\rho \simeq 6$ fm) one can approximately write

$$p^2(\rho,r') \simeq p^2(\infty,r') + \frac{a(r')}{\rho} . \tag{3.15}$$

If we choose $\langle p^2(\rho,r')\rangle = p^2(\infty,r')$ and ignore the r' dependence of $p^2(\infty,r')$, then we can replace (3.14) by

$$G_3[E-\epsilon_d-p^2(\rho,r')/2\mu_3] \approx N_3 G_3[E-\epsilon_d-p^2(\infty)/2\mu_3] , \tag{3.16}$$

where

$$N_3 = 1-i\{M_3/2[E-p^2(\infty)]\}^{1/2} a(r') . \tag{3.17}$$

Naturally, the coefficient N_3 can easily be incorporated in integral (2.3), even if we keep the r' dependence of $a(r')$.

Alternatively, one could try to parametrize the r' behavior of $p^2(\rho,r')$ in Eq. (3.14) and ignore its ρ dependence. However, the partial wave expansion of $\rho\langle \vec{r} \mid G_3 \mid \vec{r}' \rangle$ is rather more complicated than that of $\langle \vec{r} \mid G_3 \mid \vec{r}' \rangle$, so that we have not applied this option. Instead, we have considered a fairly large range of values for $\langle q^2(\rho,r')\rangle$ and N_3, so that we expect that the exact results are covered by our calculations.

IV. RESULTS

In this section we show our results for the calculation of ^{24}Mg(p,d)^{23}Mg($\frac{1}{2}^+$). In Fig. 3 we show the experimental data[10] together with the standard zero range and finite range calculations. We used the same optical potentials and neutron single particle wave functions as in Ref. 24. In Fig. 3(a) we also show the plane wave Born approximation (PWBA) calculation, which is of interest since our previous analysis showed that the exact results might be intermediate between the standard and the plane wave result. Notice that there is very little difference between the zero range and the finite range results, which include the effects of the D state. All subsequent calculations are full finite range calculations. In Fig. 4 we show the standard results and compare them with our full calculation. Also shown are the results obtained by using the standard elastic wave function for one channel, in combination with the microscopic distorted wave in the other channel. These results were obtained using the expectation values $\langle V_1 \rangle = -40$ MeV and $\langle V_3 \rangle = -15.7$ MeV. We see that the replacement of the proton elastic wave function by the microscopic distorted wave leads to a decrease of the cross section, although the reduction is nowhere near being sufficient to reproduce the experimental results. The analyzing power is not affected very much. The replacement of the deuteron elastic wave function by the distorted wave $\hat{\chi}_{3,\vec{k}}$ has a much more drastic effect. However, instead of the suppression expected from approximations like (3.6) or (3.8), we find an increase in the cross section. This increase can be traced back to the large size of the correction term in (2.3) so that the cancellation of this term and the elastic wave function is much less effective than is assumed by either (3.6) or (3.8).

In Fig. 5 we show the results for the optimal value of $\langle V_3 \rangle$ and N_3 as determined by Eqs. (3.14)–(3.17). Since a change in $\langle V_1 \rangle$ does not have a large effect on the results, we have kept $\langle V_1 \rangle$ fixed at -40 MeV throughout.

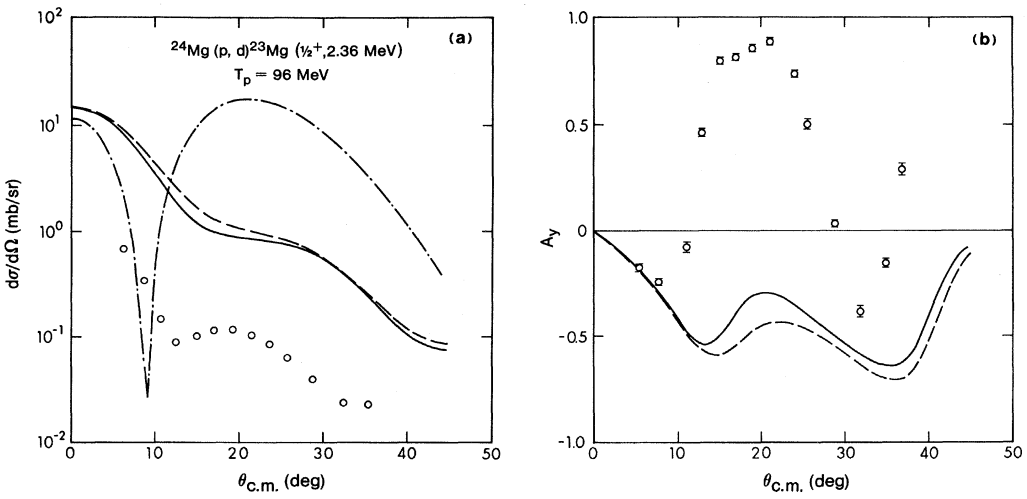

FIG. 3. Comparison of the finite range (——) and zero range (— — —) DWBA calculations with the experimental data. Also shown is the PWBA (—·—·—·) result for the cross section (the analyzing power is zero in this case).

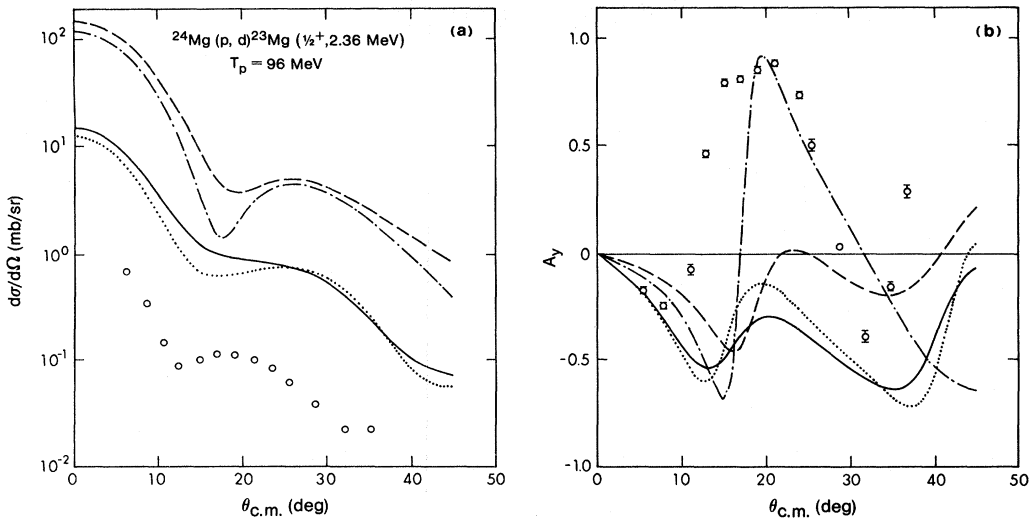

FIG. 4. Calculations using the modified distorted waves for the proton channel (· · ·), the deuteron (— · — · — ·), and for both channels (— — —) are compared with the standard calculation (——).

Both cross section and polarization improve as a result of the optimalization of $\langle V_3 \rangle$ and $\langle N_3 \rangle$. The case $\langle V_3 \rangle = -2.2$ corresponds to a value for $\langle p^2(\rho,r') \rangle \approx 0$. This is the value reached by the real part of $p^2(\rho,r')$ for large r' and ρ (see Table I). Since the PWBA result would emerge for $\langle V_i \rangle = 0$, it is not surprising that this case with small $|\langle V_3 \rangle|$ already displays some of the characteristic features of the PWBA (relatively large secondary maximum and small polarization). The variation in the results under reasonable changes in $\langle V_3 \rangle$ and N_3 is small compared to the discrepancy with experiment, so that it is likely that the first-order term cannot resolve the existing anomaly. We will discuss the implications of this result further in the next section.

Finally, it may be interesting to note that the use of Eq. (3.8) leads to a vast improvement in our results, as seen in Fig. 5. Our results are then even superior to those based on arbitrary cutoffs of Ref. 24. Although this approximation cannot be justified by our more exact results, it seems to provide a useful phenomenological description of the cutoff in the interior.

V. DISCUSSION

In this paper we presented the first practical results of a microscopic theory of transfer reactions. The modifications of the distorted waves, as demanded by theory, have been implemented and the approximations in obtaining

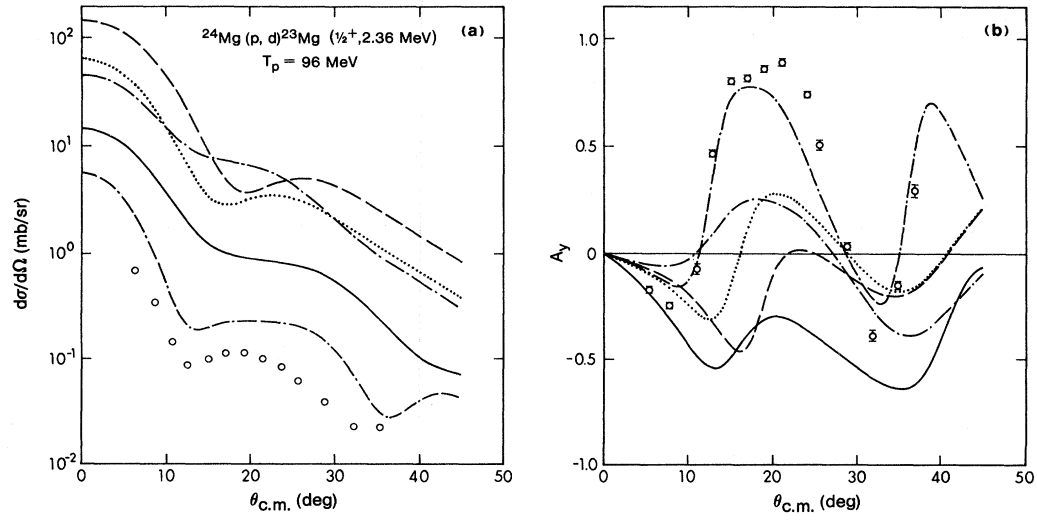

FIG. 5. Microscopic calculations using the best theoretical values for $V_3 = (-8.40, 5.14)$ and $N_3 = (1.07, -0.10)$ based on Eqs. (3.14)—(3.17) are displayed (· · ·). Also shown are results for $V_3 = -2.2$ MeV (— · — · — ·), together with the previous standard (——) and the microscopic result (— — —). The fifth curve (—— · —— · —— ·) corresponds to approximation (3.8).

practical results have been studied in some detail. We find that the (p,d) observables are very sensitive to the deuteron distorted waves and that the expected suppression of the nuclear interior is not realized in the exact calculations. The corrections to the elastic wave functions in the interior and near the nuclear surface are substantial and do not necessarily suppress the elastic wave function in the interior as was expected from the simple approximation (3.6) or (3.8).

In order to make further progress in the context of the present microscopic theory one would have to consider various refinements and extensions of the present calculations. The sensitivity to the deuteron optical potential suggests that we may have to improve its treatment. We based our analysis of $p^2(\rho,r')$ on a folding potential for the deuteron, whereas the practical calculations were based on a phenomenological deuteron optical potential. Different results for $p^2(\rho,r')$ would result if we treated the deuteron optical potential more consistently, and also incorporated breakup effects. Although we do not think that our values for $p^2(\rho',r)$ would be very much different, the use of a more microscopic deuteron optical potential could have important effects. The deuteron D state may also play an important role in the optical potential.

An important correction to our results could come from the higher-order terms in $\hat{T}_{ij}$, in particular, the rescattering term $V_i G_o T_k$, which is not suppressed by Q-space projection operators. In a previous study we showed[27] that this term by itself could explain some of the systematics of the ^{4}He(p,d)^{3}He reaction; however, a more quantitative study is necessary. Since we need a fairly strong reduction of the cross section to get agreement with experiment, one would need a strong cancellation between this term and the main DWBA diagram. This implies that an accurate calculation of the rescattering diagram is necessary. It would be preferable if we could demonstrate cancellations on the more formal level; however, we found that this could not be done in a convincing way.

Another possible improvement could result from the inclusion of the exchange term. Since Pauli effects have been shown to be small for this (p,d) reaction,[28] we would not expect that this could explain the discrepancy, although a study of this effect in the new context might be valuable.

Since these first results suggest that the first-order microscopic DWBA diagram is not sufficient to explain the (p,d) process, one might ask whether there exists an alternative microscopic theory which would fare better in the first-order term. The distorted Faddeev equations[29] would seem an obvious starting point; however, we found that the elegance of the present theory would be lost if such a starting point were used. The nonorthogonality terms arising from these distorted Faddeev equations complicate the formulation considerably and make it rather unlikely that one could accomplish the simplification of the calculation of distorted waves to a simple quadrature, which was essential for the practicality of the present theory. Nonetheless, it may be worth pursuing such a scheme further, particularly in view of recent advances made by Birse and Redish.[30]

Note added in proof: Since submitting this paper some new conventional analyses[31,32] of the process ^{24}Mg($\vec{p}$,d)^{23}Mg($\frac{1}{2}^+$) have come to my attention, indicating that the discrepancy between theory and experiment is much less than indicated in the original analysis.[24] Although these findings will not basically change the comparison between the conventional and the microscopic calculations, they do imply that it might be premature to construe the disagreement between our present calculation and experiment as a failure of the first-order term.

ACKNOWLEDGMENTS

This work was supported in part by the Natural Sciences and Engineering Research Council of Canada. We thank Dr. R. Gourishankar and C. Land for assistance with the numerical work.

[1]S. D. Baker *et al.*, Phys. Lett. 52B, 57 (1974).
[2]T. S. Bauer *et al.*, Phys. Lett. 67B, 265 (1977).
[3]J. Berger *et al.*, Lett. Nuovo Cimento 19, 287 (1977).
[4]J. Källne and A. W. Obst, Phys. Rev. C 15, 477 (1977).
[5]J. M. Cameron *et al.*, Phys. Lett. 74B, 31 (1978).
[6]J. Källne *et al.*, Phys. Rev. Lett. 41, 1638 (1978).
[7]G. Bruge, J. Phys. (Paris) 40, 635 (1979).
[8]T. S. Bauer *et al.*, Phys. Rev. C 21, 757 (1980).
[9]J. Källne *et al.*, Phys. Rev. C 21, 675 (1980).
[10]D. W. Miller *et al.*, Phys. Rev. C 26, 1793 (1982); 20, 2008 (1979).
[11]N. S. Cragie and C. Wilkin, Nucl. Phys. B14, 477 (1969); C. Wilkin, J. Phys. G 6, 69 (1980).
[12]E. Rost and J. R. Shepard, Phys. Lett. 59B, 413 (1975).
[13]E. Rost, J. R. Shepard, and D. A. Sparrow, Phys. Rev. C 17, 1513 (1978).
[14]J. R. Shepard, E. Rost, and G. R. Smith, Phys. Lett. 89B, 13 (1979).
[15]A. Tékou, Nuovo Cimento 54A, 25 (1979); J. Phys. G 7, 1439 (1981).
[16]J. R. Shepard and E. Rost, Phys. Rev. Lett. 46, 1544 (1981); Phys. Rev. C 25, 2660 (1983).
[17]A. Boudard *et al.*, Phys. Rev. Lett. 46, 218 (1981).
[18]L. D. Ludeking and J. P. Vary, Phys. Rev. C 27, 1967 (1983).
[19]J. M. Greben and F. S. Levin, Phys. Rev. C 20, 437 (1979).
[20]F. S. Levin and J. M. Greben, Phys. Rev. Lett. 41, 1447 (1978).
[21]J. M. Greben, Phys. Rev. C 25, 446 (1982).
[22]H. Feshbach, Ann. Phys. (N.Y.) 5, 357 (1958); 19, 287 (1962).
[23]F. S. Levin, in *Reaction Dynamics*, edited by F. S. Levin and H. Feshbach (Gordon and Breach, New York, 1973).
[24]J. R. Shepard *et al.*, Phys. Rev. C 25, 1127 (1982).
[25]G. H. Rawitscher and S. N. Mukherjee, Phys. Lett. 110B, 189 (1982).

[26]C. M. Perey and T. G. Perey, At. Data Nucl. Data Tables 17, 1 (1976).
[27]J. M. Greben, in Proceedings of the Workshop on Nuclear Structure with Intermediate-Energy Probes, Los Alamos Scientific Laboratory Report LA-8303-C, 1980, p. 402.
[28]R. C. Johnson, N. Austern, and M. H. Lopes, Phys. Rev. C 26, 348 (1982).
[29]E. F. Redish, Phys. Lett. 90B, 188 (1980); Gy. Bencze and E. F. Redish, Central Research Institute for Physics, Budapest Report KFKI 1979-64, 1979.
[30]M. C. Birse and E. F. Redish, submitted to Nucl. Phys. A; M. C. Birse, submitted to Phys. Rev. C.
[31]K. Hatanaka *et al.*, Talk presented at the International Symposium of Light Ion Reaction Mechanisms, Osaka, 1983.
[32]J. R. Shepard (private communication).